Bulletin of Engineering Geology and the Environment (2025) 84:470
https://doi.org/10.1007/s10064-025-04517-3

ORIGINAL PAPER

Mitigating the effect of specimen size on uniaxial compressive rock strength using a generalised correction and experimental testing method

Marek Brabec[1] · **Juraj Štetiar**[1] · **Lukáš Krmíček**[1]

Received: 9 August 2024 / Accepted: 21 September 2025 / Published online: 7 October 2025

Abstract

Uniaxial compressive strength is one of the key characteristics of rocks, typically determined by laboratory-controlled destruction of cylindrical specimens. Previous studies have found that the diameter and length-to-diameter ratio of the specimen affect the obtained strength value. The current understanding of the diameter effect is not convincing, and thus considering the low variability of extracted core sizes, the effect can be neglected. The length-to-diameter ratio effect is more distinct and, hence, it represents the main component of the correction models. Previously established corrections of the ratio effect differed in the reference ratio value corresponding to the assumed unaffected strength value. In our paper we propose a new generalised and fully variable correction method built around a single parameter plateauing equation with an additional parameter controlling the target ratio value. In addition to this correction, we also propose a new experimental testing method for unaffected uniaxial compressive strength determination using a set of rock specimens with variable length-to-diameter ratio.

Keywords Length-to-diameter ratio · Specimen size · Uniaxial compressive strength · Fractured core · Rock mechanics

Introduction

Uniaxial compressive strength (commonly abbreviated as *UCS*) is a basic characteristic of rock mass, essential to most geotechnical designs. It is defined as the highest stress which the tested rock can withstand before failure without any radial confinement of the specimen. The strength is usually determined in a uniaxial compressive test or estimated from other material properties, such as Schmidt rebound hardness (e.g. Katz et al. 2000; Wang et al. 2017; Aladejare et al. 2021). The *UCS* value also serves as the criterion for classification of rock mass in engineering applications (e.g. Hoek and Brown 1997).

For the determination of the objective and unaffected *UCS* values, the testing method has to be standardised. Therefore, the uniaxial compressive test protocol is formally defined by recognised Engineering organisations and societies, i.e. American Society for Testing and Materials (ASTM D7012-23 2023), International Society for Rock Mechanics (ISRM suggested method by Fairhurst and Hudson 1999) and German Society for Geotechnics (Mutschler 2004). All methodologies use a cylindrical rock sample with minimal diameter equal to 10–20 times the diameter of the largest mineral grain or particle. According to the ASTM D7012-23 (2023) protocol this criterion would normally be met by a sample with a diameter of about 47 mm. The ISRM method (Fairhurst and Hudson 1999) requires a minimum diameter of approximately 50 mm. The German Society for Geotechnics recommendation (Mutschler 2004) allows even for specimens with diameters as small as 30 mm (when the largest grain criterion is met). The length of the sample is defined by a length-to-diameter ratio (*L/D*, sometimes also height-to-diameter ratio, *H/D*), which should range between 1.5 and 2.5 according to the German Society for Geotechnics recommendation (Mutschler 2004), 2.0 and 2.5 according to ASTM D7012-23 (2023) and between 2.0 and 3.0 according to the ISRM suggested method (Fairhurst and Hudson 1999). However, as natural rock massifs are

✉ Marek Brabec
marek.brabec.mb@gmail.com

[1] Institute of Geotechnics, Faculty of Civil Engineering, Brno University of Technology, Brno 602 00, Czech Republic

usually intersected by structures and joints, the rock cores obtained from the borehole survey may not allow for the preparation of specimens with a sufficient length. In these cases, lower length-to-diameter ratio samples have to be tested, which potentially results in affected strength values that are not representative and thus incomparable with the results of the standardised tests. Nonetheless, the specimen size effect on the uniaxial compressive strength could be reduced or mitigated by using a correction or a specialized testing procedure.

The main objectives of our study are: (1) to optimise the correction of the length-to-diameter ratio effect for use on fractured rock cores limiting the possible specimen length and (2) to generalise the correction for different reference ratios.

Length-to-diameter ratio influence on the sample failure

Difference in length-to-diameter ratio significantly alters the failure pattern of the rock specimen (with the diameter kept constant) as it changes the proportion of influencing factors. The key factors are mainly the end-face friction effect and the presence of natural defects (Qi et al. 2022).

The end-face friction effect is based on the lateral confinement of the specimen ends by the frictional force between the specimen and the testing device platen (Qi et al. 2022). The friction force inhibits the development and expansion of microscopic cracks (Li et al. 2021), which therefore affects the stress and strain fields in the tested specimen, and thereby also the rock failure pattern (e.g. Turk and Dearman 1986; Gao et al. 2018; Chen and Chemenda 2020). The friction effect is strongest nearby the specimen ends/bases, hence it significantly influences the samples with lower length-to-diameter ratio (Fig. 1a). Due to the lower specimen volume, the presence of natural defects does not significantly affect the failure. This combination of factors usually leads to a complex failure (Tang et al. 2000) with many tensile fractures running almost parallel to the sample axis (Zhao et al. 2022).

At slightly higher ratios (Fig. 1b), the sample failure is still partially affected by the friction effect. The end-face parts of the sample are confined by the friction force (Gao et al. 2018), which therefore locally inhibits the crack development. The middle part of the specimen is untouched by the friction force effect and can deform freely. Theoretically, the fractures should therefore follow a failure plane inclined by an angle *α* (dependent on the internal shear angle of the rock), which connects both sample bases (Tuncay et al. 2019). However, the combined influence of the mentioned factors typically results in stress redistribution and a conical failure pattern (Qi et al. 2022), generally described as an hourglass shape.

As the ratio is further increased above certain limit value dependent on the rock type (Tuncay et al. 2019), the number of occurring inhomogeneities theoretically increases and therefore the presence of natural defects becomes the dominant factor (Qi et al. 2022). With the friction effect nullified in the central part of the sample, the fractures can propagate unimpeded. The typical shear failure plane is usually oriented diagonally, which for the higher-than-limit ratio surfaces at the cylindrical sample shell (Fig. 1c).

The *L/D* effect on failure pattern can greatly influence the determined values of rock properties, such as uniaxial compressive strength, modulus of elasticity or Poisson's ratio (e.g. Thuro et al. 2001 or Sujatono 2023). The highest *UCS* values are obtained from tests on samples with *L/D* ratio lower than 1.0, as more energy is necessary for the fracture propagation due to the inhibiting effect of friction force on crack development (Tuncay et al. 2019). Lengthening of

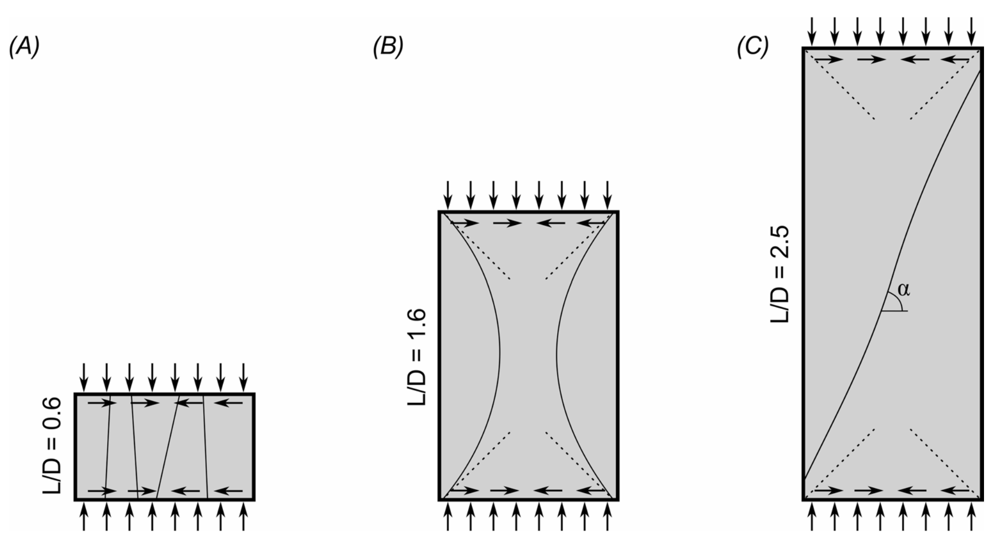

Fig. 1 Length-to-diameter ratio influence on the specimen failure pattern during uniaxial compressive test, with the friction force induced confinement near the specimen end-faces marked. (**A**) Complex tensile failure of low *L/D* sample affected by the friction induced confinement near platens. (**B**) Hour-glass failure, result of a stress redistribution caused by the friction induced confinement. (**C**) Pure shear failure of a sample with high *L/D*. Shear failure plane angle *α* defined as $45° + \varphi/2$, where *φ* is internal shear angle of the rock type

the specimen results in lower determined value of strength, the decrease of *UCS* values is usually significantly slower above ratio of 2.0 (e.g. Zhao et al. 2022).

Previously established corrections of L/D effect on UCS value

In the past, there have been several approaches to correct the effect of length-to-diameter ratio on uniaxial compressive strength of rock (see Table 1).

Some of the first widely accepted correction equations were presented in Obert et al. (1946), Obert and Duvall (1967) and Protodyakonov (1969). Turk and Dearman (1986) also presented a general correction gained by averaging the Protodyakonov (1969) equation with other previous data. Further research in the *L/D* effect correction was also conducted by Thuro et al. (2001) and Yang et al. (2005). All of the aforementioned corrections were designed with $L/D = 2.0$ as a reference value (except for Obert et al. 1946 with the reference ratio equal to 1.0) and had no further variable parameters. The correction presented by Obert and Duvall (1967) is also recommended by the German Society for Geotechnics (Mutschler 2004).

Tuncay and Hasancebi (2009) then presented a correction equation defined around the reference length-to-diameter ratio of 2.5, which is the higher value recommended in ASTM D7012-23 (2023). This equation contains two parameters, which can be varied according to the corrected rock type (for the data presented by Tuncay and Hasancebi 2009; the parameter ranges are <1.2,1.26> for *a* and <0.08,0.1> for *b*).

Latest addition to the collection of corrections was presented by Tuncay et al. (2019), who devised a sophisticated correction equation with the limit *L/D* value as a reference. The theoretical limit length-to-diameter ratio is dependent on internal friction angle, therefore variable for different rock types. For the purpose of the correction, the limit ratio can be correlated from Brazilian indirect tensile strength and/or Hoek Brown m_i constant of the tested rock type. The authors also devised a set of recommended *L/D* intervals based on the two mentioned rock type parameters for correct preparation of cylindrical specimens for uniaxial compressive testing.

Table 1 Previously established corrections of the size effect on uniaxial compressive strength with different reference length-to-diameter ratios (L/D_{ref})

Source	L/D_{ref}	Correction equation
Obert et al. 1946	1.0	$UCS^* = UCS/(0.778 + 0.222 \times (D/L))$
Obert and Duvall 1967	2.0	$UCS^* = 8 \times UCS/(7 + 2 \times (D/L))$
Protodyakonov 1969	2.0	$UCS^* = UCS/(0.875 + 0.25 \times (D/L))$
Turk and Dearman 1986	2.0	$UCS^* = 1.15 \times UCS/(1 + 0.3 \times (D/L))$
Turk and Dearman 1986	2.0**	$UCS^* = UCS \times D^{0.18}/(1.754 + 0.535 \times (D/L))$
Thuro et al. 2001	2.0	$UCS^* = UCS \times (0.925 + 0.036 \times (L/D))$
Yang et al. 2005***	2.0	$UCS^* = UCS/\exp(-0.181 + 0.397/(L/D))$
Tuncay and Hasancebi 2009	2.5	$UCS^* = UCS/(a - b \times (L/D))$
Tuncay et al. 2019	L/D_{lim}	$UCS^* = UCS \times (0.238 \times (L/D)/(L/D_{lim}) + 0.7553)$

**Equation includes diameter correction with $D_{ref} = 50$ mm; ***for marble

Abbreviations: *UCS** corrected strength value, *UCS* measured strength value, *a,b* correction parameters, L/D_{lim} limit ratio based on m_i and tensile strength of the rock, *D* specimen diameter

Additional effect of sample diameter on the measured strength

Several previous studies also addressed the necessity to correct the use of samples with non-standard diameters, however, with significantly differing results.

Hoek and Brown (1980) compared the laboratory results of uniaxial compressive tests performed on samples of various diameters up to 200 mm made of different rock types. The smaller diameter sample tests resulted in significantly higher *UCS* values and vice versa. The trend can be possibly explained with higher presence of defects in samples with larger diameter (Hoek and Brown 2019). This weakens the sample and contributes to a through-going failure formation.

Turk and Dearman (1986) pointed out the difference in results of Hoek and Brown (1980) and some previous studies (e.g. Hodgson and Cook 1970), where the influence of diameter on *UCS* value is ambiguous. They also presented a possible combined correction of both diameter and length-to-diameter ratio on strength value (see Table 1).

Thuro et al. (2001) evaluated the diameter effect on uniaxial compressive strength and deformation characteristics of granite, kersantite and limestone. For length-to-diameter ratio of 2.0, the resulting trends showed almost no dependence of the rock properties on specimen diameter.

Kahraman and Alber (2006) investigated the diameter effect on breccia consisting of partly weathered and/or altered slate clasts with calcareous cement. The prepared specimen diameters ranged from 7.5 to 100 mm. Highest uniaxial compressive strength values were determined on samples with diameter around 7.5 mm. Increasing the specimen diameter up to 40 mm leads to rapid decrease in determined compressive strength to around 20% of the highest value. With diameters larger than 40 mm, the measured compressive strength value remains almost constant.

Komurlu (2018) tested the diameter effect on various natural Turkish rock types and artificial rocklike materials. Cylindrical specimens made of natural rock had diameters of 32 and 54.7 mm with *L/D* = 2, the rocklike specimens had diameters of 26, 54 and 100 mm with *L/D* = 2. All datasets showed the same trend where tests of samples with larger diameters resulted in lower strength. Komurlu (2018) also presented a possibility of combating the diameter effect with the test performed under strain control, increasing the rate proportionally to the diameter of the specimen.

Zhai et al. (2020) conducted experimental research of the diameter effect on Gambier limestone and an artificial rock made of sand and plaster mixture. The limestone sample diameters ranged from 25 to 285 mm, the artificial rock diameter range was from 26 to 139 mm. For both sets, the uniaxial compressive strength trend peaked at a certain diameter (120 mm for limestone, 50 mm for artificial rock). For smaller diameters the compressive strength value declines rapidly, whereas for larger diameters the decreasing trend is more gradual.

Durmeková and Ondrášik (2012) and Durmeková et al. (2022) also conducted several experiments on rock specimens with variable diameters. Most of the experiments showed almost no influence of sample diameter on the determined compressive strength value. However, two sets of samples made of andesite and sandstone with length-to-diameter ratio of 1.0 showed increase in *UCS* value with larger diameters on range between 20 and 70 mm.

Practical applications with limited access to intact rock material

In geotechnical investigations, exploratory and reconnaissance borehole drilling is a standard procedure during the initial design phases. The primary objective of this drilling is to extract cores that provide continuous information about the subsurface composition (i.e. direct determination of geomaterial type and genesis, mapping of discontinuities, etc.). The extracted cores can then be tested using various laboratory methods (standard destructive tests or estimated from index properties – see Aladejare et al. 2021) to determine the intact rock properties. These values are then adjusted to account for the influence of discontinuities using indices such as the Geological Strength Index (GSI; Hoek and Brown 2019) or Rock Quality Designation (RQD; Deere 1963).

Analysing the rock core is a critical step in understanding the subsurface conditions. Typical core extracted during a geotechnical investigation is usually significantly affected by the discontinuities in the massif (see Fig. 2), which inhibits the possibility of longer samples preparation (therefore lowers possible *L/D* ratio). If the *UCS* determined on the produced low *L/D* sample is used e.g. for classification of the rock mass into categories (e.g. R0 to R6 according to Hoek and Brown 1997), the *UCS* value requires meticulous correction and adjustment.

Even if the rock core is relatively intact, producing longer samples (i.e. with L/D between 2.5 and 3.0; upper bound of the range recommended by ASTM D7012-23 (2023) and Fairhurst and Hudson 1999) is often not economical or feasible due to the larger amount of material required. Therefore, maintaining a practical approach with an *L/D* ratio of 2.0 (minimal recommended value) is usually the best compromise between material consumption and obtainment of reliable test results. The ratio of 2.0 also corresponds with the specimen requirements of the Hoek Cells used for conventional triaxial testing (*CTT*). When used for failure envelope determination along with *CTT* results, *UCS* value cannot be corrected separately as the *L/D* effect was also proven in the triaxial tests (Moomivand and Vutukuri 1996).

Fig. 2 Example of an extracted migmatite core section with prevailing discontinuities limiting the possible length of a prepared cylindrical specimen

Methodology

The proposed correction design characteristics

The presented correction model was designed for practical use in smaller geotechnical laboratories. According to the authors practise, most prepared cylindrical specimens have a diameter between 40 and 60 mm. As these values range around the recommended value of 50 mm and with taking into account the mixed results of studies focused on the diameter effect on *UCS*, the diameter of the sample was not considered in the correction. The main purpose of this correction is therefore mitigation of the *L/D* effect.

Most of the previously established correction equations used a reference length-to-diameter ratio of 2.0, which is the lower bound of usable ratios recommended by the established methodologies (i.e. Fairhurst and Hudson 1999; ASTM D7012-23 2023). Exception from this statement is Tuncay et al. (2019) equation based around a limit ratio dependent on the rock type. The proposed approach to the new correction is to predict the theoretical limit *UCS* value unaffected by the *L/D* effect through a suitable equation with a plateau. Tested equations are listed below:

$$Y = (Y_m \cdot x)/(K + x) \tag{1}$$

$$Y = (K + x)/(Y_m \cdot x) \tag{2}$$

$$Y = Y_m - (Y_m - Y_0) \cdot e^{-Kx} \tag{3}$$

Equations (1) and (2) are based on the Michaelis-Menten model used for prediction of maximum enzyme velocity, where Y_m is a maximum/minimum value (i.e. plateau) and K is a constant equal to x-value for $Y_m/2$. Both equations function as a set with opposite trends (i.e. growth and decay). Equation (3) is a plateaued exponential function with both growth and decay trends incorporated, where Y_0 is a starting value, Y_m is a plateau value and K is a rate constant.

Input data and equation selection for fitting

Total of 30 datasets used for the correction model calibration have been collected from previously published studies (i.e. John 1972; Thuro et al. 2001; Mogi 2007; Tuncay and Hasancebi 2009; Tuncay et al. 2019; Závacký 2020 and Zhao et al. 2022). Igneous rocks are represented by three granite, trachyte, lamprophyre (kersantite), two basalt, four andesite, gabbro and syenite datasets. Sedimentary rocks (including minor volcano-sedimentary rock types) are represented by dolomite, three sandstone, two limestone, two siltstone, tuff, gypsum, two ignimbrite, marlstone and greywacke datasets. Three marble datasets represent the metamorphic rock group. Uniaxial compressive strength range of the whole analysed data is from 10 to 440 MPa with 73% of the datasets under 100 MPa and 90% under 200 MPa (see Fig. 3). The uniaxial compressive tests have been carried out on samples with a diameter of 40 to 50 mm in all cases. The length-to-diameter ratio ranges for most collected datasets from 1.0 to 3.0, with one dataset including the whole range from 0.5 to 6.0 *L/D*.

The gathered datasets have been fitted with Eqs. (2) and (3) for prediction of the theoretical limit uniaxial compressive strength value. Two example datasets have been chosen to depict the difference between both models (see Fig. 4). Equation (2) trend fits all datasets relatively well regardless of the number of specimens (coefficient of determination R^2: mean = 0.886; median = 0.920; minimum = 0.576; maximum = 0.988) and does not fail to produce a limit *UCS* prediction (obtained as a reciprocal value of parameter Y_m). Equation (3) relatively well fits most of the datasets

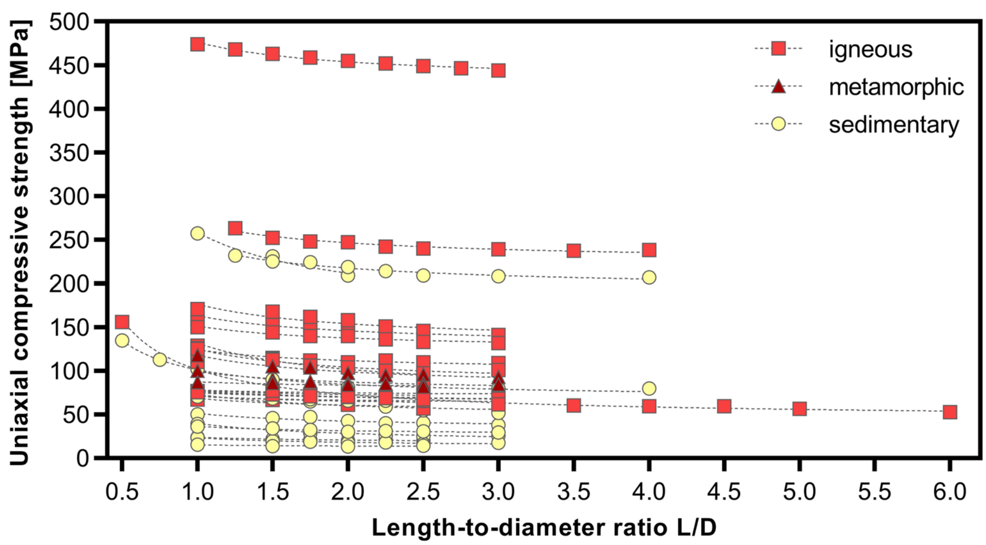

Fig. 3 Datasets collected from literature used for the correction model calibration, dashed lines represent individual fits with the proposed Eq. (2)

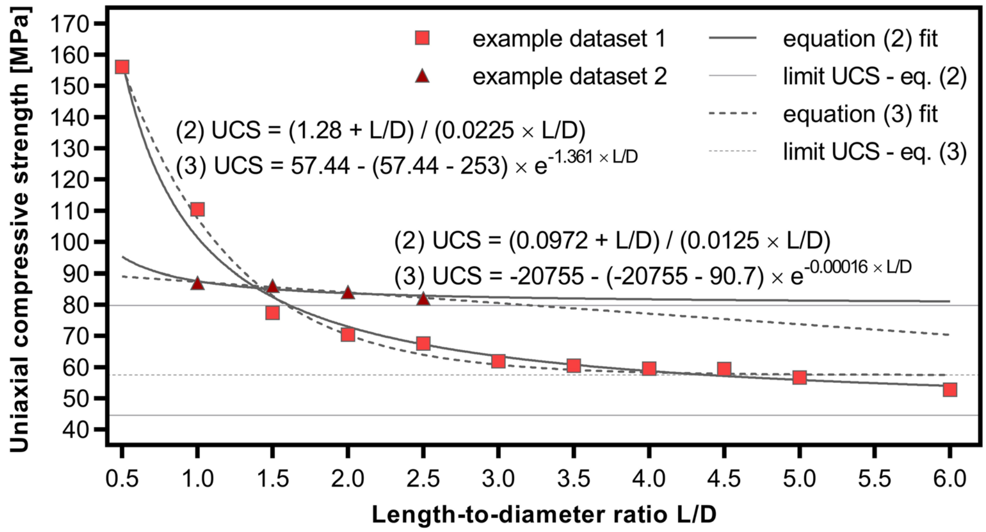

Fig. 4 Comparison of the tested equations prediction of the theoretical limit *UCS* value

including example 1 (Fig. 4) and produces a limit *UCS* value (equal to Y_m), which is higher than some of the high *L/D* points and also the prediction gained from Eq. (2). However, it fails to predict the limit *UCS* for example 2 (Fig. 4) and six other datasets. Therefore, the set of Eqs. (1) and (2) was chosen for the correction model as it is proven reliable for the gathered data. The possible disadvantage of this equation is the lower predicted limit *UCS* value, which can be further corrected with additional parameter.

Correction model derivation and calibration

The input data were fitted with Eq. (2) to determine parameters Y_m and K for each dataset with predicted UCS_{lim} values calculated as $1/Y_m$. The K parameter value therefore corresponds to the length-to-diameter ratio, for which the *UCS* value equals twice the value of UCS_{lim}. A set of strength values corresponding to the fitted curve was then calculated for each dataset, with *L/D* ranging from 0.5 to 6.0 with 0.5 step. As the datasets number of values vary significantly, thanks to the usage of the calculated values, all datasets are equally represented in the correction. Next, the limit *UCS* values for each dataset were divided by the calculated values to obtain a set of correction coefficients. These coefficient values were all then plotted and fitted with Eq. (1) both as individual sets and as one general set (see Fig. 5). The plateau (Y_m) was constrained to 1.0 to ensure that the theoretical limit value would remain unchanged. The K values for individual datasets correspond to the initial *UCS* value fits. The general correction fit shows a moderately strong positive correlation with $R^2 = 0.5419$ and K value = 0.3468 (95% confidence interval: 0.3217 to 0.3727; all datasets with corresponding K values are presented in Table 2).

A possibility of multiple separate corrections for igneous, sedimentary and metamorphic rock types (as is commonly done, e.g. Demirdag et al. 2018) was also investigated.

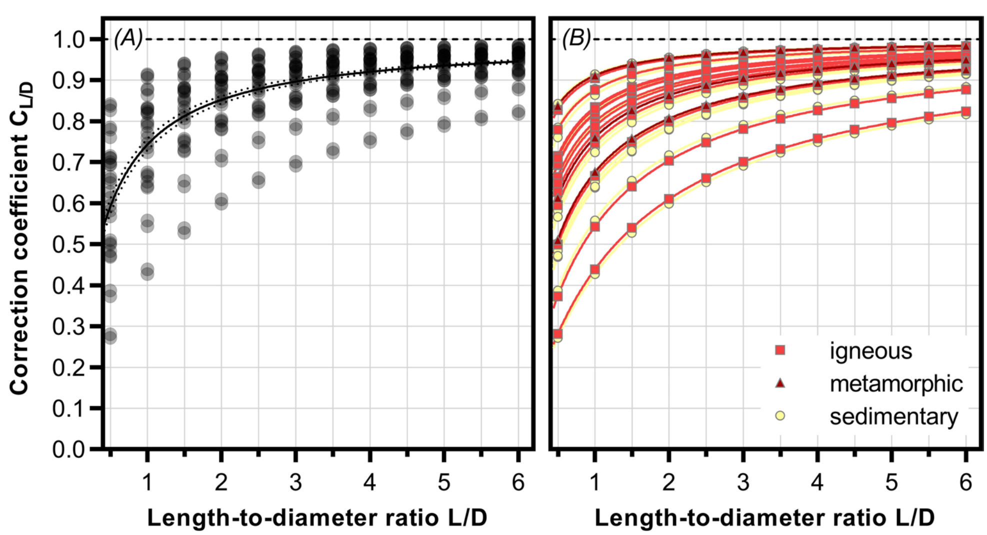

Fig. 5 The correction coefficient datasets plotted and fitted. (**A**) General correction fit (full line represents the best fit; dotted line represents the 95% confidence interval). (**B**) Individual dataset fits, sorted according to the rock type genesis

Table 2 Input datasets used for the correction model calibration with Hoek-Brown constant estimates based on the rock type (m_i*), correction parameters (K) and predicted limit uniaxial compressive strength values (UCS_{lim})

Rock type	Genesis	Source	m_i*	K	UCS_{lim}
andesite	igneous	Tuncay et al. 2019	25	0.205	63.33
andesite	igneous	Tuncay et al. 2019	25	0.220	63.45
andesite	igneous	Tuncay and Hasancebi 2009	25	0.142	65.66
andesite	igneous	Tuncay and Hasancebi 2009	25	0.841	71.63
basalt	igneous	Tuncay and Hasancebi 2009	25	0.297	52.80
basalt	igneous	Tuncay et al. 2019	25	0.502	83.19
gabbro	igneous	Tuncay et al. 2019	27	0.341	131.63
granite	igneous	Zhao et al. 2022	32	1.279	44.48
granite	igneous	Tuncay et al. 2019	32	0.222	123.92
granite	igneous	Mogi 2007	32	0.199	224.06
kersantite	igneous	Thuro et al. 2001	30	0.105	431.22
syenite	igneous	Tuncay et al. 2019	30	0.270	128.58
trachyte	igneous	Mogi 2007	30	0.253	99.30
dolomite	sedimentary	Mogi 2007	9	0.260	192.38
greywacke	sedimentary	Závacký 2020	18	0.567	164.85
gypsum	sedimentary	Tuncay et al. 2019	7	0.791	13.00
ignimbrite	sedimentary	Tuncay et al. 2019	30	0.382	26.35
ignimbrite	sedimentary	Tuncay et al. 2019	30	0.137	62.15
limestone	sedimentary	Tuncay and Hasancebi 2009	9.5	0.157	67.57
limestone	sedimentary	Tuncay et al. 2019	9.5	0.094	71.43
marlstone	sedimentary	Tuncay et al. 2019	7	0.359	17.61
sandstone	sedimentary	Tuncay et al. 2019	17	0.534	33.44
sandstone	sedimentary	Tuncay et al. 2019	17	0.560	46.99
sandstone	sedimentary	John 1972	17	0.494	67.84
siltstone	sedimentary	Tuncay et al. 2019	7	1.341	17.00
siltstone	sedimentary	Tuncay and Hasancebi 2009	7	0.203	59.28
tuff	sedimentary	Tuncay and Hasancebi 2009	13	0.214	12.55
marble	metamorphic	Tuncay et al. 2019	9	0.316	75.30
marble	metamorphic	Tuncay and Hasancebi 2009	9	0.097	79.74
marble	metamorphic	Tuncay et al. 2019	9	0.480	79.81

However, the gathered data did not indicate the influence of the rock genesis or type on *K* values as the intervals overlap.

To expand the usability of the presented correction model, an idea of modifying the equation with a coefficient to obtain a corrected *UCS* value corresponding to a different reference length-to-diameter ratio was also explored. Ratios of 2.0, 2.5 and 3.0 were chosen, as these values are the bounds of the *L/D* ranges recommended by the mentioned standards and could therefore be desired. First, the *UCS* values for the target *L/D* ratios were calculated from the dataset fits and divided by the limit *UCS* values. Next, a dependence of the obtained *UCS* ratio on the correction parameter *K* was investigated. In all three cases, there is a very strong correlation ($R^2 = 1.0$) between the *UCS* ratio and the *K* value. Therefore, only a simple linear equation was necessary for definition of the coefficient with Y-intersect equal to 1 and slope *a* controlling the target *L/D* value. The assembled a calibrated correction model is presented in Eq. (4) and visually as a nomogram in Fig. 6.

$$UCS_{cor} = UCS \cdot C_{L/D} = UCS \cdot (1 + a \cdot K) \cdot (L/D)/(K + L/D) \tag{4}$$

where UCS_{cor} is corrected uniaxial compressive strength value; *UCS* is laboratory determined uniaxial compressive strength value; $C_{L/D}$ is correction coefficient; *a* is parameter controlling the target *L/D* value (0 for the limit value; 0.333 for $L = 3D$; 0.4 for $L = 2.5D$; 0.5 for $L = 2D$); *K* is correction parameter affecting the overall trend – 0.3468 for all tested rock types (with 95% confidence interval: 0.3217 to 0.3727; *K* values for the tested rock types are presented in Table 2); *L/D* is the tested sample length-to-diameter ratio.

Possible different approach to the size effect mitigation

The correction model is not the only method for mitigation of size effect of the laboratory specimens on measured uniaxial compressive strength of rock. The possibility of direct experimental laboratory determination of unaffected *UCS* value using a specimen set with variable *L/D* fitted with the presented Eq. (2) was further explored.

Results and discussion

Practical application of the presented correction model

The basic application of the presented correction would be a simple calculation of the unaffected/limit *UCS* value using Eq. (4) with parameter *K* equal to the general best-fit value

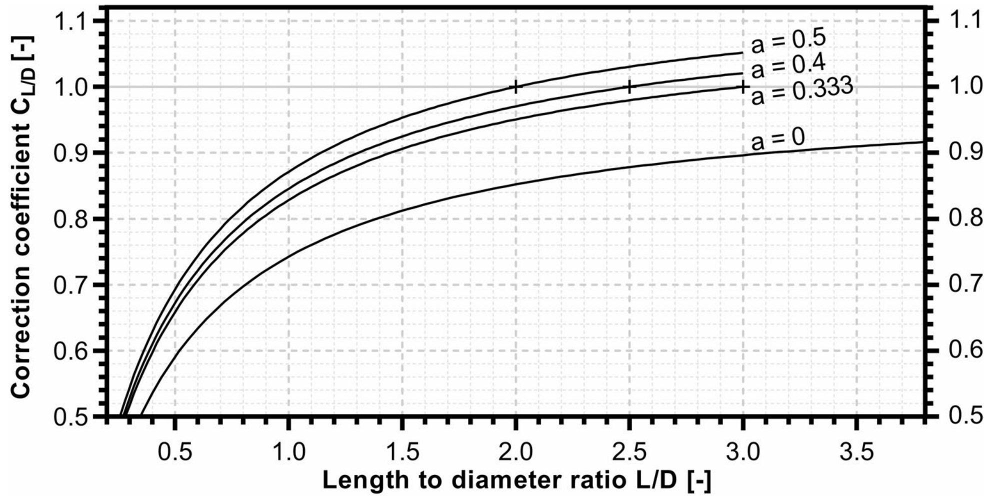

Fig. 6 Nomogram of the presented correction (for $K = 0.3468$) with different target *L/D* ratios controlled by parameter *a*

(0.3468). As this procedure always reduces the strength of the rock, the correction therefore behaves as a safety factor. Many tested rock types can be corrected in this manner as the individual *K* values are relatively close to the best-fit, leading to tolerable deviations. To demonstrate the correction effect, a sample with low length-to-diameter ratio was prepared from the extracted core (see Fig. 2) and tested in uniaxial compression. The *UCS* value was then used for determination of approximate Hoek-Brown failure criterion and rock classification. This simulates a preliminary geotechnical survey during initial stages of design with a limited access to rock material. The m_i constant was estimated according to Marinos and Hoek (2001), influence of *GSI* and *D* was negated to simulate intact rock mass. The rock classification was done according to Hoek and Brown (1997). As presented in Fig. 7, the applied correction lowered the *UCS* value from 112 to 82 MPa, which also caused a shift in the rock grade from R5 to R4.

Some of the datasets (e.g. one siltstone and granite set) show significantly higher *K* values (even above 1.0; see Table 2). Correction of these datasets using the best-fit *K* value would therefore produce significant deviations in the obtained *UCS*. For a more customised approach to the particular rock type, the *K* value can be estimated. However, the *K* value does not seem to be rock type specific (e.g. range for andesite is from 0.14 to 0.84; see Table 2), nor does it correlate with other rock type parameters, such as m_i constant. This fact complicates the estimation, which is why all of the available rock types and matching *K* values were presented in Table 2 to help the potential user. The authors advise using the best-fit *K* value as a starting point, which can then be modified according to the presented values to better suit the target rock type. Proper execution of this procedure may lead to more accurate correction in contrast to the general equation. However, caution is necessary as the estimation of *K* value may also lead to more pronounced over or underestimation the strength.

Comparison of the proposed correction model with previously established equations

The limit *UCS* prediction capabilities of the newly derived correction model presented in Eq. (4) were tested on the 30 available rock datasets and compared with results of the correction model based on limit *L/D* value (Tuncay et al. 2019). All values were normalised with uniaxial compressive

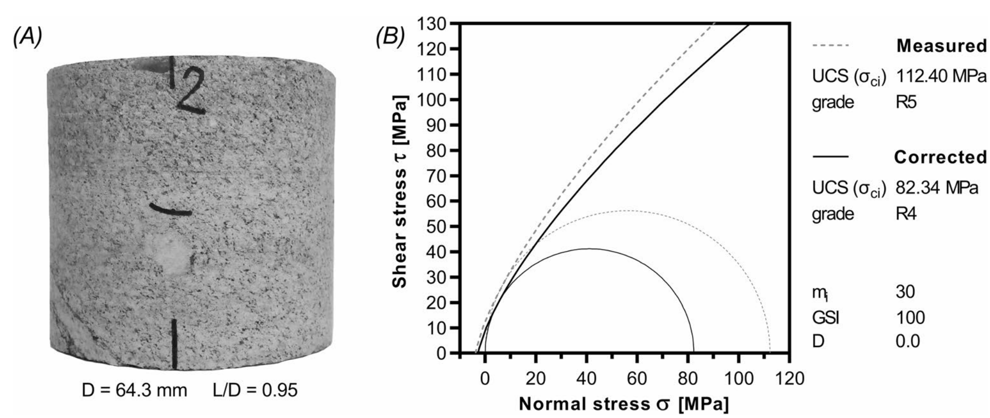

Fig. 7 Simple application of the presented correction. (**A**) Migmatite sample cut from the core presented in Fig. 2 and tested in uniaxial compression. (**B**) Hoek-Brown failure criterion approximated from the sample *UCS* value, with estimated m_i based on the rock type and in laboratory conditions (without the influence of *GSI* and *D*). Note that the correction of the *UCS* value also causes a difference in the derived rock type grade

strength values determined in laboratory on samples with *L/D* = 2.0 (referenced to as *UCS* ratio). The *L/D* ratio of 2.0 (lower bound value recommended by Fairhurst and Hudson 1999 and ASTM D7012-23 2023) was chosen as all datasets included a corresponding specimen and most previous corrections used it as a reference. The values of the presented correction model coefficients were selected to correspond with the general correction variant (i.e. $K = 0.3468$) without any constraint to the *UCS* prediction (i.e. $a = 0$ to obtain the limit value). First step of the limit *L/D* model application was estimation of m_i value for the limit *L/D* calculation, which was done according to Marinos and Hoek (2001) based on the dataset rock type (see Table 2). The correction was then applied to samples with *L/D* lower than the limit value, the rest of the samples were left uncorrected. The measured values and values corrected using both models were then plotted in Fig. 8 as mean *UCS* ratio values with standard deviations, separately for all datasets. The three *UCS* ratio sets were also summarised in separate relative frequency plots (Fig. 8) with mean values and standard deviations calculated to determine more generalised trend of the corrections. The measured values correspond to 102.8 ± 13.7% of the *UCS* value for *L/D* = 2.0, the limit *L/D* model (Tuncay et al. 2019) results in correction to 94.7 ± 9.6% and the proposed limit *UCS* model corrects the measured values to 85.4 ± 5.9%. Both correction models lower the deviation of the whole dataset, with the proposed model being almost twice as effective. As for the mean value, the proposed model results in 10% lower general *UCS* ratio than the second model. This difference could be corrected by changing the coefficient *a* value from 0 to 0.333 (therefore correcting to reference *L/D* = 3.0). After this modification, the *UCS* ratio value rises to 95.3 ± 6.6% of the *UCS* value for *L/D* = 2.0, which practically corresponds to the second model range, only with lower deviation.

Most of the previously established correction models were based around a reference *L/D* = 2.0 (see Table 1). As mentioned before, the presented correction model can be easily modified for different target/reference *L/D* value using the coefficient *a*. The modified correction model ($K = 0.3468$; $a = 0.5$) was compared with one of the previously established models (i.e. Obert and Duvall 1967) for evaluation of this modification. The comparative correction was applied only to samples with *L/D* < 2.0, according to German Society for Geotechnics recommendation (Mutschler 2004). All values were normalised with uniaxial compressive strength values determined in laboratory on samples with *L/D* = 2.0 as in the previous case. The data were then plotted in Fig. 9 as mean *UCS* ratio values with standard deviations, separately for all datasets and also summarised in relative frequency plots. Uncorrected values correspond to the previous case (i.e. 102.8 ± 13.7%). The chosen comparative correction (Obert and Duvall 1967) results in 5% decrease of deviation with mean value closer to the expected 100% (i.e. 99.3 ± 8.1%). The presented correction model proves to be slightly more effective as the *UCS* ratio mean value shifts to 100.2% with prominent decrease of deviation to 6.9%.

Based on the experiments, the presented correction model seems to be relatively versatile with two specimen size mitigation modes. First correction mode ($a = 0$) relies on unaffected *UCS* value prediction based around the plateauing trend of the used equation. The second correction mode with variable target/reference *L/D* can be controlled using coefficient *a* to simulate specific conditions. To obtain an approximate limit *UCS* value comparable with previous model, a target *L/D* = 3.0 (i.e. $a = 0.333$) seems to provide reliable results. Changing reference *L/D* to 2.0 (i.e. $a = 0.5$) enables correction of *UCS* value for usage in some specific applications (e.g. in combination with Hoek Cell triaxial tests for failure envelope determination). The presented

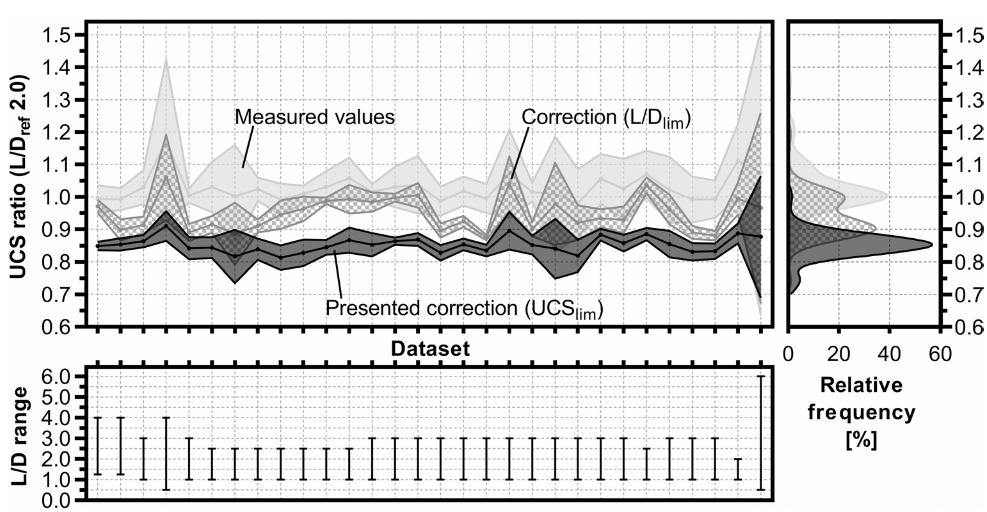

Fig. 8 Comparison of the presented correction based on limit *UCS* prediction with previously established correction based on the limit *L/D* value (Tuncay et al. 2019). Measured and corrected *UCS* values in each dataset were divided with corresponding *UCS* values determined on samples with *L/D* = 2.0 to calculate *UCS* ratio. Mean values and standard deviations of *UCS* ratio were plotted for each dataset, as well as *L/D* ranges. All datasets are also summarised in relative frequency plots for both corrections and measured values

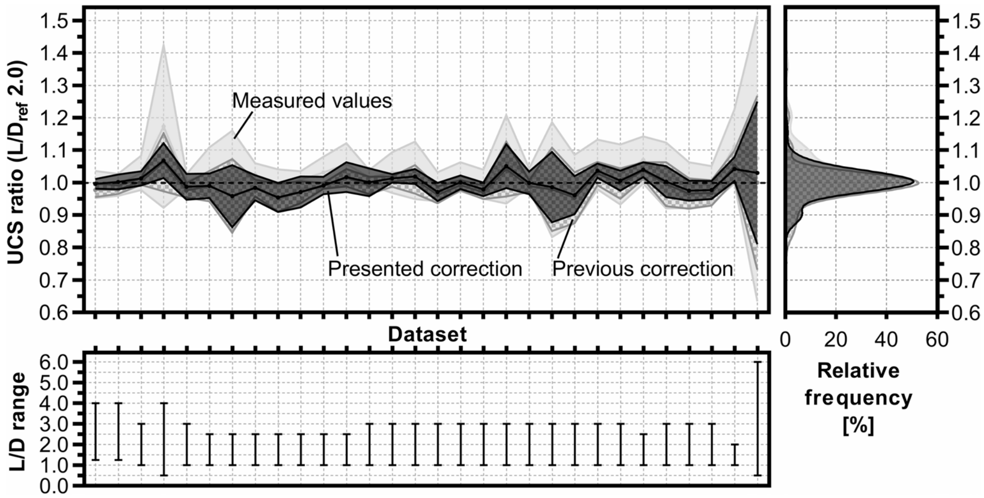

Fig. 9 Comparison of the presented correction modified to predict *UCS* corresponding to *L/D* = 2.0 with previously established correction (Obert and Duvall 1967) recommended by the German Society for Geotechnics. Measured and corrected *UCS* values in each dataset were divided with corresponding *UCS* values determined on samples with *L/D* = 2.0 to calculate *UCS* ratio. Mean values and standard deviations of *UCS* ratio were plotted for each dataset, as well as *L/D* ranges. All datasets are also summarised in relative frequency plots for both corrections and measured values

model even offers lower deviations than the comparative model specialised for correction to *L/D* = 2.0 (Obert and Duvall 1967).

Experimental determination of UCS_{lim} and K on a set of samples with variable L/D

Discontinuities in rock massifs usually impede extraction of longer cores. However, production of specimens with lower *L/D* could still be possible even with fractured cores. In this case, the authors suggest assembling a set of samples with variable length-to-diameter ratio and testing them in uniaxial compression. Obtained dataset could then be fitted with Eq. (2) to determine K and UCS_{lim} values specific for the tested rock type.

To evaluate this procedure, a set of samples was prepared from a coarse biotite granite (see Fig. 10a) sampled in Moldanubian batholith. The selected granite shows a slight separation of light and dark minerals, forming so-called leucocratic parts. The samples were tested in uniaxial compression with load rate of 1000 N/s and the results plotted as a dependence on *L/D*. The overall granite dataset trend (see Fig. 10b) corresponds with the trend of the presented model, however, failure of the last specimen with *L/D* ≈ 3.1 was affected by a slightly weaker plane with higher presence of dark minerals. The natural defect was not apparent during core examination, but its presence resulted in atypical failure pattern and lower *UCS* value differing from the expected trend. As mentioned in the introduction, the longer specimens are more affected by the natural defects as the friction induced confinement is only influencing the end-faces of the specimen. Other four samples correspond with typical failure patterns (Fig. 1), showing a transition from hourglass-like pattern at *L/D* ≈ 2.1 to tensile failure with vertical fractures at lower ratios. The granite dataset was used for creation of four sub-datasets with different *L/D* ranges (0.6–3.1, 0.6–2.1, 0.6–1.1 and 0.6–0.9; see Fig. 11) to study the optimal specimen set composition for reliable

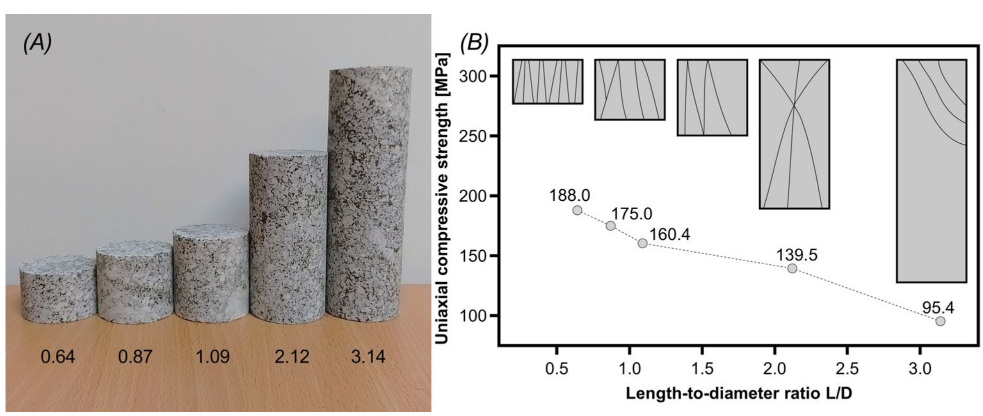

Fig. 10 (**A**) Specimens made of granite sampled in Moldanubian batholith. (**B**) Results of the granite samples tested in uniaxial compression with failure sketches

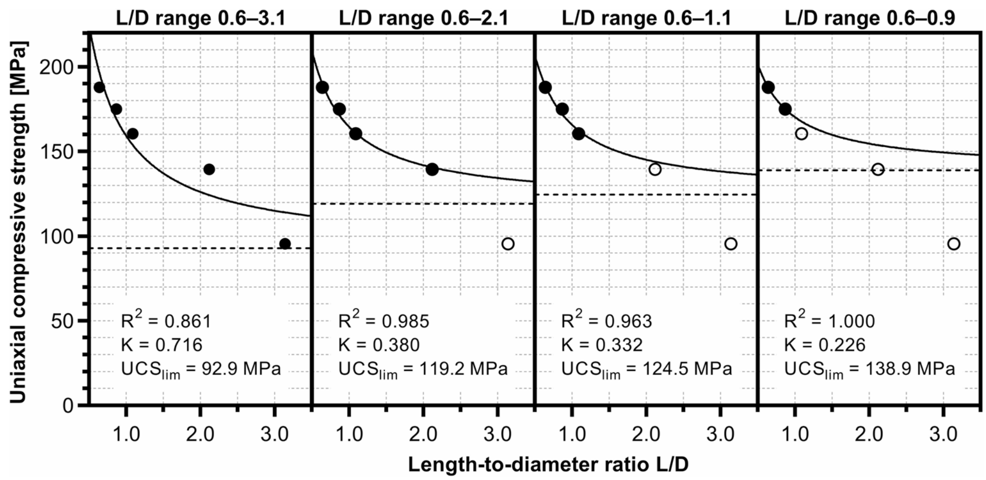

Fig. 11 Demonstration of *L/D* range effect on the experimentally determined limit *UCS* and *K* value of the tested granite. Fitted values are displayed as full circles, limit strength value is marked with dashed line

unaffected *UCS* prediction. Therefore, the sub-datasets were fitted with Eq. (2) to determine UCS_{lim} and *K* values (see Fig. 11). The widest set fit was significantly affected by the invalid *UCS* value for the longest specimen, which notably lowered the predicted strength and goodness of fit. Sub-sets with *L/D* ranges of 0.6–1.1 and 0.6–2.1 both resulted in reliable strength predictions with high R^2. The last sub-set, with only two specimens and low *L/D* range, significantly overestimated the predicted *UCS* value.

To confirm the optimal set composition, the only two datasets from the cited literature containing samples with $L/D<1.0$ were also analysed (granite from Zhao et al. 2022 in Table 3 and sandstone from John 1972 in Table 4). From the analysed datasets, minimal conditions for reliable unaffected *UCS* prediction were deduced: specimen set must be comprised of at least three specimens, two of them can have *L/D* lower than 1.0, with the third having *L/D* equal to 1.5 or more. In case of the sandstone dataset, even two specimens with *L/D* range of 0.5–0.75 gave reliable prediction (however, this is most likely an isolated case which cannot be relied on).

The unaffected *UCS* value is usually significantly lower, than even values determined on samples with high *L/D* recommended by the methodologies (2.5 according to ASTM D7012-23 2023 and 3.0 according to Fairhurst and Hudson 1999). As the *L/D* ratio for these predictions of unaffected *UCS* is theoretically approaching infinity, it may be desirable to obtain *UCS* values more in line with standard test results. This procedure results in obtaining both UCS_{lim} and *K* values, therefore *UCS* corresponding to any *L/D* can be calculated using these values and Eq. (2). The procedure may be even more enhanced with incorporation of the limit *L/D* theory by Tuncay et al. (2019), which results in the final methodology of the proposed experimental testing method: Specimen set comprised of three samples (two with $L/D<1.0$ and one with $L/D\geq1.5$) at minimum would be tested in uniaxial compression. Results of the tests would be then plotted in *UCS* dependence on *L/D* ratio and fitted with curve based on Eq. (2) to obtain *K* and Y_m parameters ($Y_m = 1/UCS_{lim}$). Next, m_i would be estimated according to Marinos and Hoek (2001) for calculation of L/D_{lim}. Final step of the procedure is calculation of unaffected *UCS* value using Eq. (2) and L/D_{lim} as *x*. The whole process was demonstrated in Fig. 12 on the three available datasets (Moldanubian granite dataset, granite dataset from Zhao et al. 2022 and sandstone dataset from John 1972) with suitable specimen composition. Only three samples were chosen for the fit according to the authors recommendation with the rest also plotted. The last modification results in 10 to 15 MPa

Table 3 Study of a necessary set composition for reliable prediction of unaffected uniaxial compressive strength of a granite (Zhao et al. 2022) using the presented equation

Samples	L/D range	UCS range	R^2	K	UCS_{lim}
11	0.5–6.0	53–156	0.987	1.280	44.5
10	0.5–5.0	57–156	0.986	1.269	44.7
9	0.5–4.5	60–156	0.985	1.275	44.6
8	0.5–4.0	60–156	0.985	1.300	44.0
7	0.5–3.5	60–156	0.984	1.316	43.7
6	0.5–3.0	62–156	0.982	1.321	43.6
5	0.5–2.5	68–156	0.979	1.299	44.0
4	0.5–2.0	70–156	0.975	1.316	43.7
3	0.5–1.5	77–156	0.965	1.210	46.2
2	0.5–1.0	110–156	1.000	0.707	64.7

Table 4 Study of a necessary set composition for reliable prediction of unaffected uniaxial compressive strength of a sandstone (John 1972) using the presented equation

Samples	L/D range	UCS range	R^2	K	UCS_{lim}
8	0.5–4.0	80–135	0.988	0.494	67.8
7	0.5–3.0	80–135	0.994	0.522	66.3
6	0.5–2.5	79–135	0.996	0.543	65.2
5	0.5–2.0	81–135	0.995	0.538	65.5
4	0.5–1.5	90–135	0.999	0.494	68.0
3	0.5–1.0	102–135	1.000	0.478	69.0
2	0.5–0.75	113–135	1.000	0.478	69.0

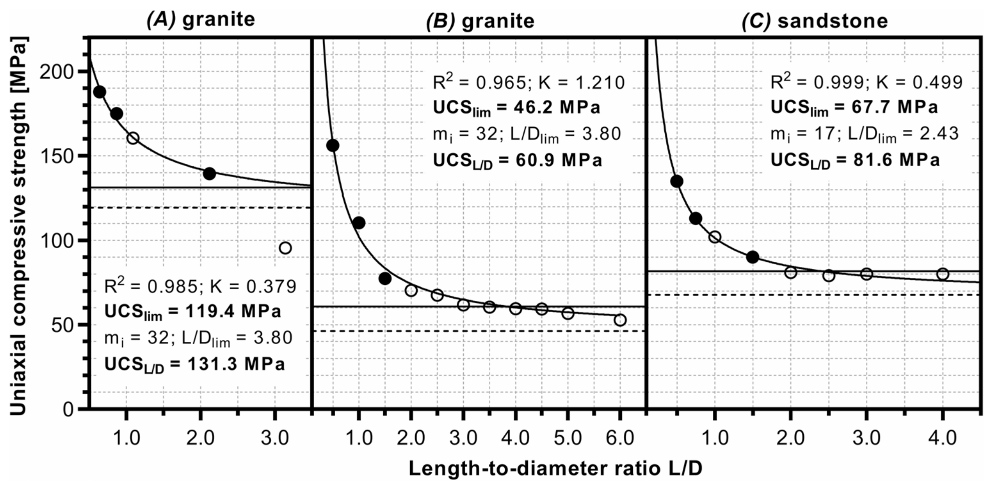

Fig. 12 Evaluation of experimental unaffected *UCS* determination method with incorporation of limit *L/D* theory (Tuncay et al. 2019). Fitted values are displayed as full circles, predicted limit strength value UCS_{lim} is marked with dashed horizontal line and modified limit value $UCS_{L/D}$ calculated using limit *L/D* is marked with full horizontal line. (**A**) Granite sampled in Moldanubian batholith. (**B**) Granite dataset from Zhao et al. (2022). (**C**) Sandstone dataset from John (1972)

increase of the unaffected *UCS* value against the equation-only predicted value. The modified predicted value seems to be more realistic when compared with the high *L/D* sample results from the examined datasets.

Further comments and notes for future research

The presented correction model and experimental testing method for mitigation of rock specimen size effect proved to be relatively reliable. The correction was derived and tested on 30 datasets of various rock types and genesis gathered from the available literature dealing with the topic. However, before more widespread use, the model should be further verified on additional datasets with incorporation of the missing rock types, mainly other metamorphites. The experimental testing method was tested only using three datasets as the other ones did not include samples with *L/D* < 1.0, with two of them being various granites and the third made of sandstone. The test results suggest that the method is reliable, mainly with incorporation of the limit *L/D* theory (Tuncay et al. 2019). When the available rock core is significantly fractured, this method allows for use of shorter specimens with only some of them meeting the minimal *L/D* requirements. Analysis and comparison of the specimen failure with the theoretical crack patterns also seems to be useful for verification of the individual sample tests (e.g. rejection of the invalid sample with *L/D* = 3.14 in Fig. 10b). However, the presented experimental method should be further verified on additional datasets with emphasis on weaker rock types. Weaker rocks may be problematic due to the variability of the mass and higher presence of natural defects (such as foliation or porosity), which could interrupt proper determination of the *L/D* trend crucial for the experimental testing method. Finally, the proposed correction model and experimental testing procedure should be also verified for use on a saturated rock mass. The premise is that the presented general equation should be still valid for saturated rocks, only expected modification is usage of slightly different *K* value.

The equation used in both the correction and the experimental testing method is controlled by a main parameter *K*, which significantly varies across the available datasets (from 0.09 to 1.34). The correction model operates reliably with the generalised *K* value (e.g. see comparison with previous correction in Fig. 9). However, if the *K* value could be easily determined or correlated for the specific rock types, it could significantly enhance the correction performance. Authors tried to find a suitable correlation between the *K* value and other available parameters (such as estimated m_i value, uniaxial compressive strength for commonly available *L/D* ratios, rock type or genesis). However, no clear and usable correlation was found as the *K* value can significantly vary even for the same rock types (e.g. range for andesite is from 0.14 to 0.84; see Table 2). The *K* value could theoretically depend on more complex characteristics of the rock material, such as grain size, composition (e.g. quartz vs. matrix content for sediments) or a degree of weathering. (1) Variable grain size: With increasing predominant mineral grain size, the internal friction angle should increase and therefore also the failure plane angle – this could result in higher variation between shorter (*L/D* ~ 0.6) and longer (*L/D* ~ 3.0) specimens, and thereby higher *K* value. Additionally, the grain size could also affect the stress distribution in the specimen, becoming more heterogeneous for coarser rocks, thus further affecting the *K* value. (2) Differing mineral composition: Example case for clastic sediments could be variable quartz content – hardness and stiffness of the rock could increase with higher quartz content, possibly resulting in more pronounced end-face friction effect for shorter specimens (*L/D* ~ 0.6), thus increasing the *K* value. On the contrary, with prevailing component being the matrix, it can reduce the rocks strength and its ability to strengthen with the end-face confinement and therefore lower the *K* value. (3) Weathering: With progressive weathering and alteration of the mineral components, the softer grains may crumble and be partially replaced by the secondary products, thus increasing porosity, lowering strength, grain size and/or intergranular cohesion, directly impacting the *K* value. Apart from the rock characteristics, the *K* value controlling the *L/D* correction could also be affected by the testing conditions, such as loading rate. Theoretically, the increased loading rate could alter the failure mechanism and the obtained strength value, possibly also the strength difference between variably long specimens and thus the *K* value. Another factor could possibly be variation between stress-controlled and strain-controlled loading, which is why we recommend strict adherence to the typical loading rates recommended by the ASTM D7012-23 (2023) and ISRM (Fairhurst and Hudson 1999) for standardisations of the *K* value determination. Apart from the structural properties, even the level of saturation can affect the obtained *K* value, as mentioned before. Important factors to be defined: (A) Lowering of the effective stress: as the pores and cracks in rock mass become saturated, the water bears part of the applied stress in form of the pore pressure, resulting in reduction of the effective stress, weakening of the intergranular bonds and thus lowering of the overall rock strength (Fu et al. 2025) and likely affecting the *K* value. (B) Alteration of the failure mechanism: the water present in pores and cracks of a saturated rock may affect the failure mechanism, especially for longer specimens – as the pore pressure builds up with increasing applied uniaxial stress, the water could cause increased outward radial stress and microcrack propagation (Ma et al. 2023), thus promoting splitting of the specimen. As a result, the strength values determined on longer specimens could be even lower, which would lead to higher *K* value.

Additional experiments (e.g. using natural or artificial rock specimens, along with numerical simulations using grain-based models) are therefore in order, hopefully providing necessary clarification on the *K* value determination. Combination of these techniques could be beneficial as both methods have limitations. The grain-based models would allow for detailed microstructural analysis of the studied *L/D* effect, allowing for separation of individual variables and effects (which could be difficult using the physical experiments), and also facilitate a preliminary study for planning of subsequent physical experiments. The artificial rock specimens could be then prepared and tested based on the numerical study results. Different aggregate sizes (from gravel to silt or even clay) could be used to study the grain size effect on *K* value. The heterogeneous grain distribution could be simulated during specimen production using, e.g., stacked alternated finer and coarser, or porous and compact mixes. With cement-based artificial rock mix, the effect of specimen saturation on *K* value could be also determined. The artificial rock specimens would even allow for concurrent *L/D* and diameter effect study using specimens with mixed specifications. In the final step, the artificial rock results could be verified on various natural rock types to obtain full understanding of individual effects controlling the *K* value.

The authors would also like to highlight another possibility of mitigating the effect of specimen size during the uniaxial compressive test indicated in previously published research. As mentioned before, the major factor responsible for the shape effect is confinement of the specimen end-faces caused by the friction force between the rock sample and the steel platen. Theoretical and experimental results (Yang et al. 2005; Pan et al. 2009) proved, that negation of the friction should eliminate the length-to-diameter effect on the measured *UCS* value (valid for 0.5 to 3.0 *L/D* ratio range). The end friction effect can be reduced by an application of lubricant to the contact surfaces between the specimen and testing device platens (e.g. Labuz and Bridell 1993 or Qi et al. 2022).

Conclusions

The practical application of geotechnical investigations with limited access to rock material involves optimizing the use of core samples and also ensuring that the laboratory tests are conducted in an efficient and reproducible way. By adhering to standard protocols and allowing the necessary corrections, reliable data can be obtained even with limited sample material. Our study explores the influence of specimen size on the determined uniaxial compressive strength value. Two possible methods for mitigating this effect are proposed and described.

The first proposed method is a fully variable correction model based around plateauing equation used for the unaffected *UCS* value prediction. The predicted value is generally about 10% lower than the results obtained from previous corrections or the high *L/D* specimen tests. If a more standardised *UCS* value is required, the target *L/D* ratio can be easily modified by using a correction parameter *a*. This way, the presented correction model can also replace most of the conventional models with comparable outcomes.

The second method is newly proposed experimental laboratory procedure developed on a sample set with variable *L/D* values. Fractured or jointed core samples do not usually allow for standard specimen preparation. Our proposed method involves testing of at least three samples, two of them can have $L/D<1.0$ and the third one should be closer to standards with $L/D>1.5$ or more. The dataset is subsequently plotted in *UCS* on *L/D* dependence and fitted with the proposed equation for the required *UCS* value calculation. Then a strength value corresponding to any *L/D* ratio can be calculated using the obtained equation based on the respective needs.

Acknowledgements This research was financially supported by Brno University of Technology (grant No. FAST-S-24-8658). We are indebted to Daniel Müller (Las Condes, Santiago, Chile) for his valuable advice and recommendations on the first draft of the manuscript. We greatly appreciate the suggestions and helpful comments on this manuscript from the three anonymous reviewers. We also thank the handling editor for perfect editorial work.

Funding Open access publishing supported by the institutions participating in the CzechELib Transformative Agreement.

Data availability Data available after request.

Declarations

Competing interest The authors declare that they have no known competing financial interests or personal relationships that could have appeared to influence the work reported in this paper.

References

Aladejare AE, Alofe ED, Onifade M et al (2021) Empirical estimation of uniaxial compressive strength of rock: database of simple, multiple, and artificial intelligence-based regressions. Geotech Geol Eng 39:4427–4455. https://doi.org/10.1007/s10706-021-01772-5

ASTM D7012-23 (2023) Test methods for compressive strength and elastic moduli of intact rock core specimens under varying states of stress and temperatures. ASTM International. https://doi.org/10.1520/D7012-23

Chen J, Chemenda AI (2020) Numerical simulation of true 3D rock tests with classical and new three-invariant constitutive models focusing on the end effects. Arab J Sci Eng 45:9367–9378. https://doi.org/10.1007/s13369-020-04750-w

Deere DU (1963) Technical description of rock cores for engineering purpose. Rock Mech Eng Geol 1:16–22

Demirdag S, Sengun N, Ugur I, Altindag R (2018) Estimating the uniaxial compressive strength of rocks with Schmidt rebound hardness by considering the sample size. Arab J Geosci 11:502. https://doi.org/10.1007/s12517-018-3847-1

Durmeková T, Bednarik M, Dikejová P, Adamcová R (2022) Influence of specimen size and shape on the uniaxial compressive strength values of selected Western Carpathians rocks. Environ Earth Sci 81:247. https://doi.org/10.1007/s12665-022-10373-1

Durmeková T, Ondrášik R (2012) Heterogeneity and scale effect in determination of rock strength. Min Slovaca 44:149–156

Fairhurst CE, Hudson JA (1999) Draft ISRM suggested method for the complete stress-strain curve for intact rock in uniaxial compression. Int J Rock Mech Min Sci 36:281–289

Fu T-F, Zhu D-F, Li Y-T (2025) Modeling the mechanical properties of rock at different pore and confining pressures using the grain-based stress corrosion model. Geophys J Int 241:326–337. https://doi.org/10.1093/gji/ggaf048

Gao M, Liang Z, Li Y et al (2018) End and shape effects of brittle rock under uniaxial compression. Arab J Geosci 11:614. https://doi.org/10.1007/s12517-018-3957-9

Hodgson KE, Cook NGW (1970) The effects of size and stress gradient on the strength of rock. In: Proceedings of the second congress of the international society for rock mechanics. International Society for Rock Mechanics, Belgrade, pp 31–34

Hoek E, Brown ET (1980) Underground excavations in rock. The Institution of Mining and Metallurgy, London

Hoek E, Brown ET (1997) Practical estimates of rock mass strength. Int J Rock Mech Min Sci 34:1165–1186. https://doi.org/10.1016/S1365-1609(97)80069-X

Hoek E, Brown ET (2019) The Hoek–Brown failure criterion and GSI – 2018 edition. J Rock Mech Geotech Eng 11:445–463. https://doi.org/10.1016/j.jrmge.2018.08.001

John M (1972) The influence of the length to diameter ratio on rock properties in uniaxial compression: a contribution to standardisation in rock mechanics testing. Geomech Intern Rep ME10835 1972

Kahraman S, Alber M (2006) Estimating unconfined compressive strength and elastic modulus of a fault breccia mixture of weak blocks and strong matrix. Int J Rock Mech Min Sci 43:1277–1287. https://doi.org/10.1016/j.ijrmms.2006.03.017

Katz O, Reches Z, Roegiers J-C (2000) Evaluation of mechanical rock properties using a Schmidt hammer. Int J Rock Mech Min Sci 37:723–728. https://doi.org/10.1016/S1365-1609(00)00004-6

Komurlu E (2018) Loading rate conditions and specimen size effect on strength and deformability of rock materials under uniaxial compression. International Journal of Geo-Engineering 9:17. https://doi.org/10.1186/s40703-018-0085-z

Labuz JF, Bridell JM (1993) Reducing frictional constraint in compression testing through lubrication. Int J Rock Mech Min Sci Geomech Abstr 30:451–455. https://doi.org/10.1016/0148-9062(93)91726-Y

Li S, Liu G, Jia R et al (2021) Study on friction effect and damage evolution of end face in uniaxial compression test. J Min Strata Control Eng 3:99–108

Ma D, Wu Y, Yin J et al (2023) Effect of initial pore pressure on the hydraulic fracturing of tight sandstone: an experimental study. Geomech Geophys Geoenerg Geo-resour 9:15. https://doi.org/10.1007/s40948-023-00547-x

Marinos P, Hoek E (2001) Estimating the geotechnical properties of heterogeneous rock masses such as flysch. Bull Eng Geol Environ 60:85–92. https://doi.org/10.1007/s100640000090

Mogi K (2007) Experimental rock mechanics. Taylor & Francis, London

Moomivand H, Vutukuri V (1996) Effects of Diameter-to-length ratio on the strength of cylindrical specimens in triaxial tests. Institution of Engineers, Australia, Barton, ACT

Mutschler T (2004) Recommendation 1 (revised) of the commission on rock testing of the Deutsche gesellschaft für geotechnik e. V.: uniaxial compression tests on rock samples. Bautechnik 81:825–834. https://doi.org/10.1002/bate.200490194

Obert L, Duvall WI (1967) Rock mechanics and the design of structures in rock. Wiley, New York

Obert L, Duvall WI, Windes SL (1946) Standardized tests for determining the physical properties of mine rock. U.S. Bureau of Mines

Pan P-Z, Feng X-T, Hudson JA (2009) Study of failure and scale effects in rocks under uniaxial compression using 3D cellular automata. Int J Rock Mech Min Sci 46:674–685. https://doi.org/10.1016/j.ijrmms.2008.11.001

Protodyakonov MM (1969) Method of determining the strength of rocks under uniaxial compression. Mech Prop Rocks 1–8

Qi M, Zhao G, Xu W et al (2022) Influence of height–diameter ratio on rock compressive failure characteristics and damage evolution law. Energies 15:5557. https://doi.org/10.3390/en15155557

Sujatono S (2023) Optimum length-to-diameter ratio of floatstone under uniaxial compressive strength test. Geotech Geol Eng. https://doi.org/10.1007/s10706-023-02660-w

Tang CA, Tham LG, Lee PKK et al (2000) Numerical studies of the influence of microstructure on rock failure in uniaxial compression — Part II: constraint, slenderness and size effect. Int J Rock Mech Min Sci 37:571–583. https://doi.org/10.1016/S1365-1609(99)00122-7

Thuro K, Plinninger R, Zah S, Schutz S (2001) Scale effects in rock strength properties. Part 1: unconfined compressive test and Brazilian test. Rock Mech Chall Soc 169–174

Tuncay E, Hasancebi N (2009) The effect of length to diameter ratio of test specimens on the uniaxial compressive strength of rock. Bull Eng Geol Environ 68:491–497. https://doi.org/10.1007/s10064-009-0227-9

Tuncay E, Özcan NT, Kalender A (2019) An approach to predict the length-to-diameter ratio of a rock core specimen for uniaxial compression tests. Bull Eng Geol Environ 78:5467–5482. https://doi.org/10.1007/s10064-019-01482-6

Turk N, Dearman WR (1986) A correction equation on the influence of length-to diameter ratio on the uniaxial compressive strength of rocks. Eng Geol 22:293–300. https://doi.org/10.1016/0013-7952(86)90030-X

Wang H, Lin H, Cao P (2017) Correlation of UCS rating with Schmidt hammer surface hardness for rock mass classification. Rock Mech Rock Eng 50:195–203. https://doi.org/10.1007/s00603-016-1044-7

Yang S, Su C, Xu W (2005) Experimental and theoretical study of size effect on rock material. Eng Mech 22:112–118

Závacký M (2020) Effect of length to diameter ratio on uniaxial compressive strength of rock. In: Juniorstav 2020 Proceedings. Faculty of Civil Engineering – Brno University of Technology, Brno, pp 370–374

Zhai H, Masoumi H, Zoorabadi M, Canbulat I (2020) Size-dependent behaviour of weak intact rocks. Rock Mech Rock Eng 53:3563–3587. https://doi.org/10.1007/s00603-020-02117-z

Zhao Z, Yang G, Li G, Zhang K (2022) Effects of the length–diameter ratio on the dissipation energy in the process of rock deformation and failure. Energy Rep 8:13369–13375. https://doi.org/10.1016/j.egyr.2022.10.003